Optimization of an Oil Boom Arrangement

Jianzhi Fang, Kau-Fui Vincent Wong
University of Miami
Department of Mechanical Engineering
Coral Gables, FL

The object under study is an innovative boom arrangement, consisting of a ramp boom and three other conventional booms of different drafts. In order to optimize the design, an advanced VOF (Volume of Fluid) algorithm is developed to calculate oil-water flows in the complex geometry. The effects of the gravity, current velocity and depth, spans between the conventional booms, ramp boom's draft and inclination angle, oil viscosity and density are considered in the present numerical modeling. A comparison was made between the computational simulation and the laboratory experiment of the boom arrangement, and satisfactory results were obtained.

From the numerical investigations, it is found that the oil slick flowing behind the ramp boom is similar to that of a solid object travelling under the influence of the gravity. To achieve a high performance, the ramp slope should be as small as possible and the span of the boom system should cover the oil's "landing distance". Under the tide current conditions, the simulations show that the small amplitude tide may improve the system's performance, while the large amplitude tide significantly deteriorates it. The smaller angular-frequency tide is more harmful to the system, especially if the tide's amplitude is large at the same time.

1 Introduction

To protect water intakes and harbor entrances from oil-spill pollution, permanent oil boom arrangements are usually placed around those locations to protect them, instead of a single boom (Lo, 1995, and Wong et al., 1995, 1996, 1999). Four types of barriers can retain or deflect the oil slicks: floating booms, air-bubble barriers, skimmer walls, and sorbent barriers. Based on the study of cost and effectiveness (Lo, 1995), it was found that the floating boom arrangements were the most appropriate method for protecting the intakes and harbor entrances from an oil spill.

In this paper, a specific oil boom arrangement (Wong and Kusijanovic, 1999) with a ramp boom will be studied numerically. In the next section, the performance of this boom arrangement is investigated under different current velocities. In section 3, we will focus on the effect of the ramp's slope. By studying the effectiveness of several modified designs, the calculations help to optimize the boom arrangement. In the last section, the incoming current is described by a sine wave to simulate the tide condition, which is an approximation to the real current condition encountered by oil boom arrangements.

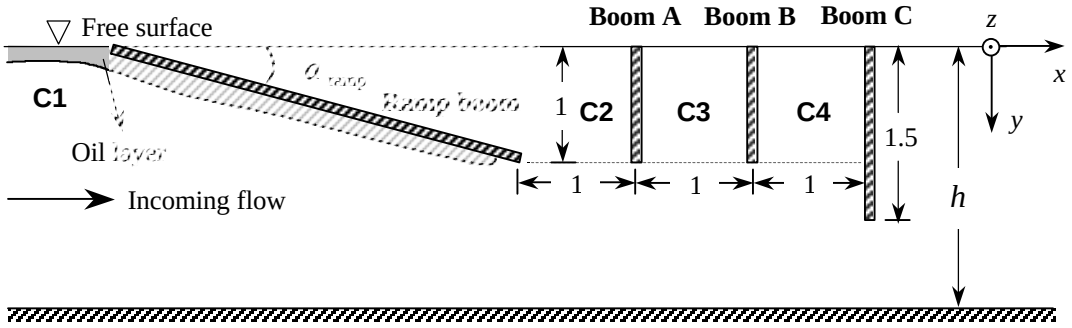

Figure 1 Configuration of a boom arrangement

The cross-sectional view of the boom system (the study object) is illustrated in Fig.1. On the upstream side there is a ramp boom with an inclination angle $a_{\text{ramp}} = 15^0$. Following the ramp boom there are three regular booms (A, B and C). In this chapter, the upstream region of the ramp boom is called the oil collection zone **C1**. The regions around the ramp boom and booms A, B and C are named the oil collection zones **C2**, **C3**, and **C4**, successively (see Fig.1). The sizes labeled in Fig.1 are dimensionless. The unit length is the draft of the boom A (or B). The widths of the booms arranged in *z* direction are the same as the span of the protection area, which is much longer than the draft of the booms. Therefore, the two-dimensional model is also valid for this study. The detail numerical scheme is discussed in Fang and Wong (1999), and Fang (2000).

2 System Performance under Different Current Velocity

The performance of the aforementioned boom arrangement has been tested in an open channel apparatus (Wong and Kusijanovic, 1999). Automotive oil was used to form an oil slick. Three regions of velocity have been found in the laboratory experiment. In the first region, where the current velocity is less than 0.15m/s, most of the oil is collected in oil collection zone **C1**. In the second region, where the current velocity is smaller than 0.20m/s, most of the oil is trapped. In the third region, where the current velocity is greater than 0.30m/s, the boom system is no longer effective in containing the oil slick.

In order to compare with the experimental results, the physical parameters in the present calculations are chosen to be the same as those in the experiment. The viscosity and density of the automotive oil are $m_{\text{oil}} = 9.5\times10^{-2}\,\text{N.s/m}^2$ and $r_{\text{oil}} = 870\,\text{kg/m}^3$. The draft of the boom A (or B) is $d = 4.5$ cm. Therefore, the dimensionless parameters are

$$s_m = \frac{m_{\text{oil}}}{m_{\text{water}}} = 79 \tag{1}$$

$$s_r = \frac{r_{\text{oil}}}{r_{\text{water}}} = 0.84 \tag{2}$$

$$\text{Re}_d = \frac{r_{\text{water}} U_0 d}{m_{\text{water}}} = 3.75\times10^4 U_0 \tag{3}$$

$$\mathrm{Fr}_d = \frac{U_0}{\sqrt{gd}} = 1.49U_0 \qquad (4)$$

where $m_{\text{water}} = 1.2 \times 10^{-3}\,\text{N.s/m}^2$, $r_{\text{water}} = 10^3\,\text{kg/m}^3$; U_0 is the current velocity in m/s. Because the interfacial tension is not important to the study of the drainage failure and the critical accumulation failure, the interfacial tension is excluded in the following simulations. Another dimensionless parameter, the depth ratio, is a constant, $h_d = 3.5$. The initial simulation conditions are of no motion. The oil slick is initially placed at the upstream side as a rectangular block. The dimensionless incoming current velocity is linearly increased from 0 to 1 over a short time after the calculation starts.

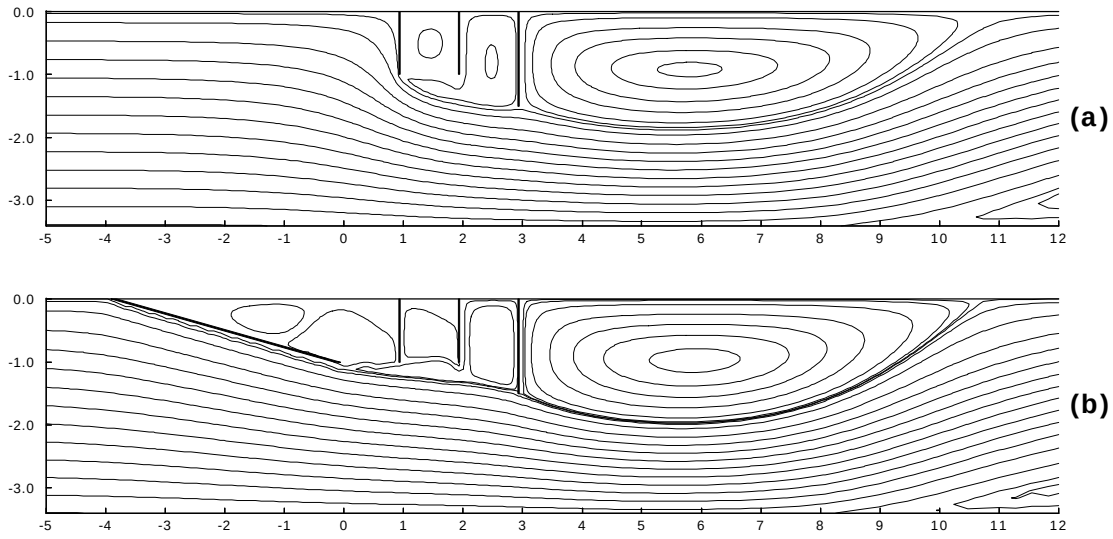

Figure 2 Streamline plots of one-fluid cases (Re = 7500)

In order to understand the function of the ramp boom, two cases have been calculated for the purpose of comparison. In Fig.2 is shown the plots of the streamlines for one-fluid flow when it reaches steady state. The case without a ramp boom is shown in Fig.2(a), while the case with a ramp boom is shown in Fig.2(b). Comparing these two plots, one can deduce that the ramp helps to trap the oil in two ways. Firstly, the ramp guides the direction of the flow. When the fluid enters the oil collection zones, it will have a lower vertical velocity, and the oil may be prevented from overshooting past these collection zones. The second reason is that with the presence of the ramp, there is a large quiescent oil collection zone behind it, which is favorable for the oil and water to stratify into stable layers under the influence of gravity.

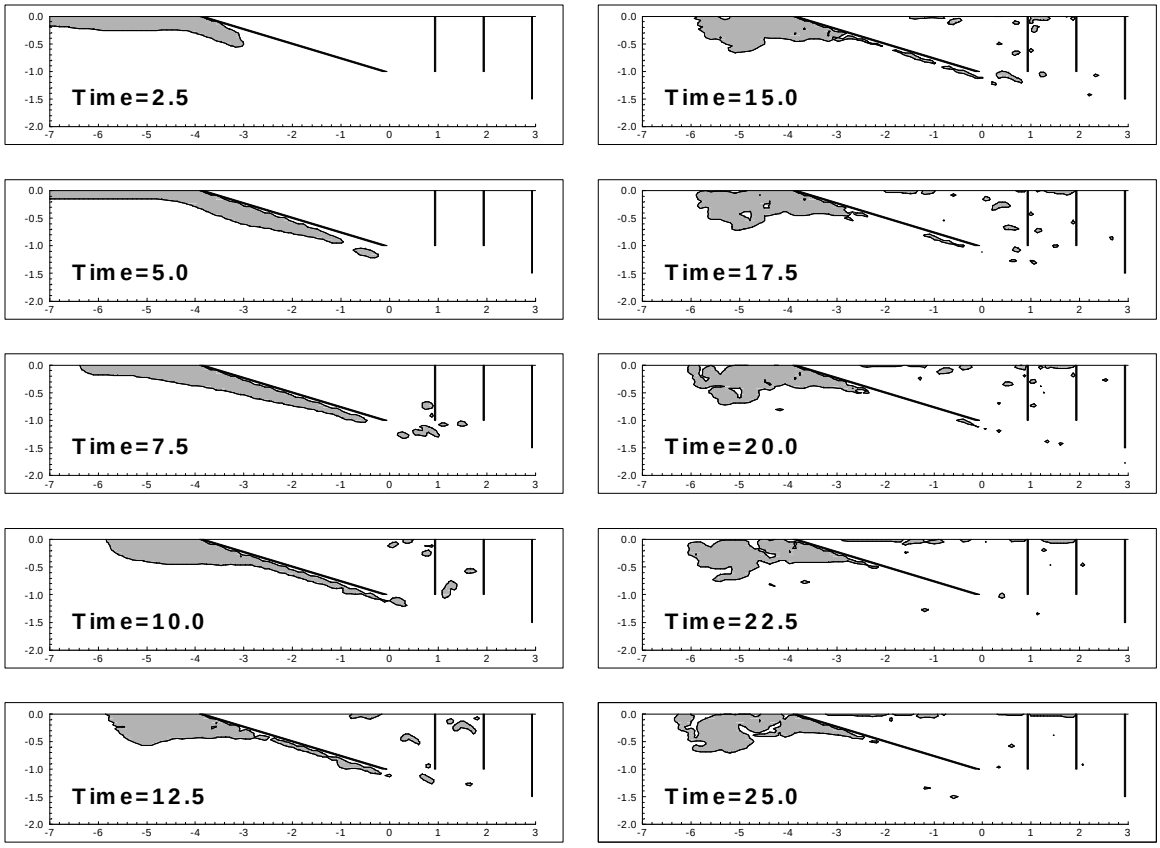

Figure 3 Evolution of the oil slick under the current velocity of 0.15m/s
Time stamped in the plots is dimensionless time. In this case, the dimensionless time 1 corresponds to 0.3 second.

In the following section, we will present and discuss the computational results of the boom arrangement retaining oil under several current velocities. With the current velocity $U_0 = 0.15$ m/s, the Reynolds number and the Froude number are $\mathrm{Re} = 5625$ and $\mathrm{Fr} = 0.2235$. It is seen from Fig.3 that along the ramp boom the oil slick moves forward at the beginning and moves backward in the last frame shown. Only a little oil enters the oil collection zones **C2** and **C3**, most of the oil stays in the collection zone **C1**. After **Time=12.5**, a headwave is seen on the tail of the oil slick. It is known that under the influence of the buoyancy force alone, an oil slick has the tendency to stretch out along the free surface; but on the tail of the oil slick, the water current pushes it forward against this stretching movement. Therefore, these two opposite actions cause the headwave.

When the current velocity increases to 0.20m/s, all the oil passes under the ramp boom, and most of the oil will be collected by this boom system. It is showed in Fig.4 that the oil is broken into pieces and the interface is totally deformed when the oil enters the collection zones. But at $\mathrm{time} = 45$, the oil finally stays on top of the zones; the oil and water are well separated again. By this point, the present computational technique has been shown to handle well the flow with complex interfaces. In the case of $U_0 = 0.30$ m/s, the oil slick moves so fast that much of the oil passes by the boom system. Only 48% of the oil has been collected by this boom system. As shown in frame **Time=10** to **Time=15** of Fig.5, the path of the oil slick is like a trajectory. It suggests that a suitable

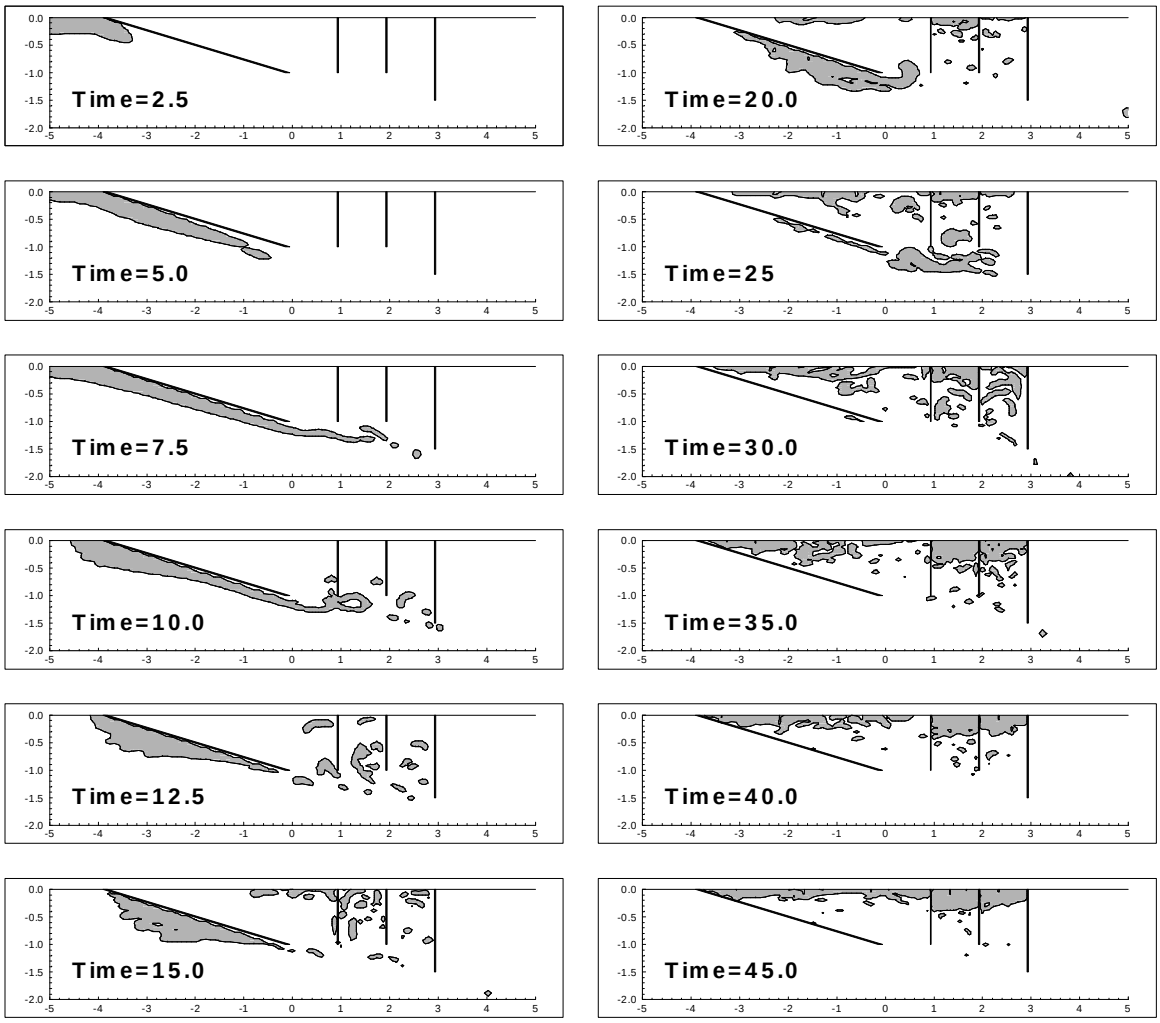

Figure 4 Evolution of the oil slick under the current velocity of 0.20m/s

Time stamped in the plots is dimensionless time. In this case, the dimensionless time 1 corresponds to 0.225 second.

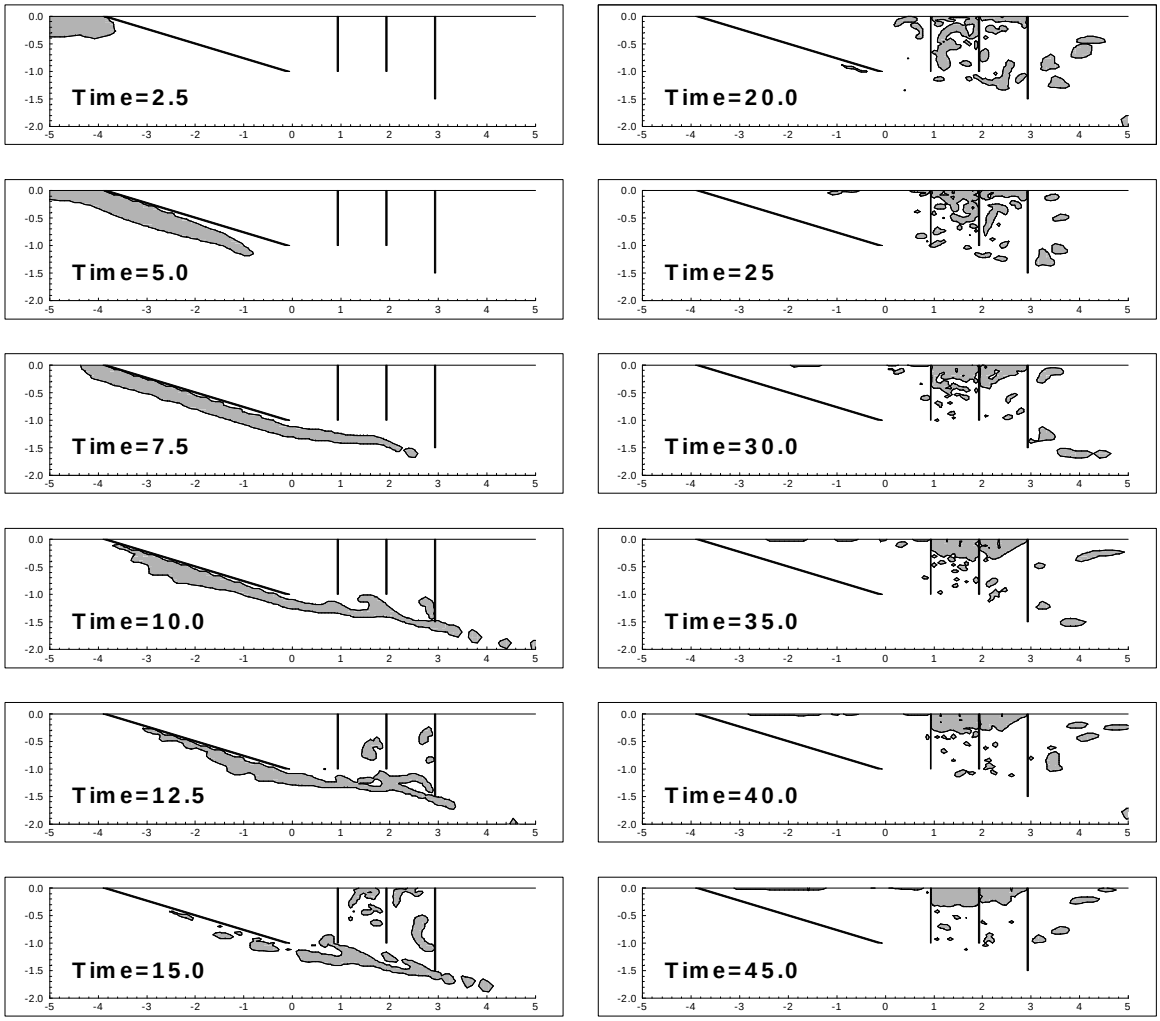

Figure 5 Evolution of the oil slick under the current velocity of 0.30m/s

Time stamped in the plots is dimensionless time. In this case, the dimensionless time 1 corresponds to 0.15 second.

ramp slope (a_{ramp}), and a longer span (d_A) between the ramp boom and boom A may ensure the oil will "land" inside the oil collection zones. From the experimental study of the two-boom configuration, Lo (1995) suggested that the span be about 16 times of the boom's draft, for each boom to act separately, so that the second boom does not interfere with the vortex behind the first boom. For a ramp boom, the velocity of the oil leaving the ramp is much lower than the velocity of the oil leaving the skirt of a conventional boom of equivalent draft. Since this is the case, we expect the span of the vortex after the ramp boom to be less than 16 times of the boom's draft, as found by Lo. This fact suggests that the spans used in the boom arrangement studied here are workable. The spans used were the same as those studied by Wong and Kusijanovic (1999), and found to be practically workable. A simple analyzed formulation is presented later, in Eqn.8.

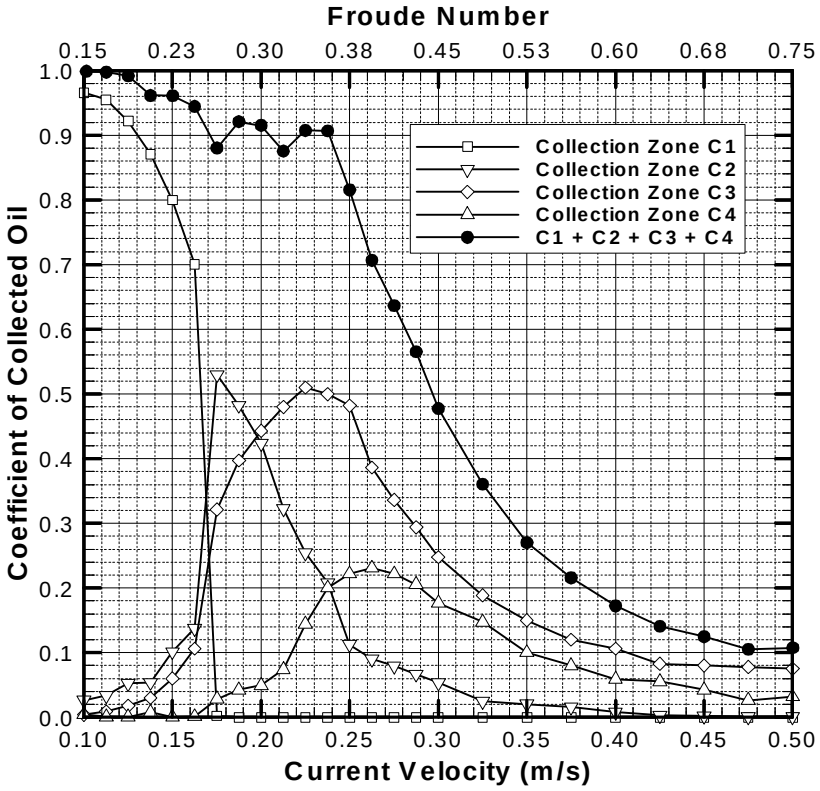

Figure 6 Coefficient of collected oil vs. the current velocity

The performance of the boom arrangement under different current velocities is illustrated with Fig.6. In the following discussion, the coefficients of collected oil contributed by the collection zones **C1**, **C2**, **C3** and **C4** are denoted by $V_{\text{oil}}^{\text{C1}}$, $V_{\text{oil}}^{\text{C2}}$, $V_{\text{oil}}^{\text{C3}}$ and $V_{\text{oil}}^{\text{C4}}$, respectively. The coefficient of collected oil is then the sum.

$$V_{\text{oil}} = V_{\text{oil}}^{\text{C1}} + V_{\text{oil}}^{\text{C2}} + V_{\text{oil}}^{\text{C3}} + V_{\text{oil}}^{\text{C4}} \tag{5}$$

As shown in Fig.6, when the current velocity (U_0) is less than 0.166m/s, or the Froude number (Fr) is less than 0.247, more than 50% of the oil is trapped in the collection zone **C1** ($V_{\text{oil}}^{\text{C1}} > 0.5$). While at $U_0 = 0.175\,\text{m/s}$ ($\text{Fr} = 0.263$), $V_{\text{oil}}^{\text{C1}}$ suddenly drops to zero. But with the presence of the other three booms in this system, the overall

performance is still very good, V_{oil} is as high as 0.88. At this point where $U_0 = 0.175$ m/s, $V_{\text{oil}}^{\text{C2}}$ reaches its maximum. When $U_0 \geq 0.30$ m/s, it is found that $V_{\text{oil}}^{\text{C2}} < 6\%$, most of the oil does not have the chance to collect in **C2** at this high current velocity. Even though we will not study the effect of the span, theoretically an appropriate span between booms is very important in a boom arrangement.

As an analogy, the oil passing under the ramp boom may be compared to a projectile being shot out of a cannon and then falling under the influence of gravity. With a fixed ramp's slope, the larger the current velocity, the longer the "landing distance" of the oil. This fact is also observed from the curves of $V_{\text{oil}}^{\text{C2}}$, $V_{\text{oil}}^{\text{C3}}$ and $V_{\text{oil}}^{\text{C4}}$. There is a peak on each curve. It may be explained that this peak occurs in an oil collection zone because the oil's "landing point" is inside this zone and here is the place for the oil to emerge to the free surface. Among **C2**, **C3** and **C4**, **C2** is the closest zone to the ramp, it is implied that the peak of $V_{\text{oil}}^{\text{C2}}$ corresponds to the shortest "landing distance". It should correspond to the smallest current velocity, according to the free-falling-object assumption. **C4** is the farthest zone to the ramp, the peak of $V_{\text{oil}}^{\text{C4}}$ occurs at the longest "landing distance", and it should have the largest corresponding current velocity. This deduction is proved by the fact presented in Fig.6. At the peaks of $V_{\text{oil}}^{\text{C2}}$, $V_{\text{oil}}^{\text{C3}}$ and $V_{\text{oil}}^{\text{C4}}$, the current velocities are 0.175m/s, 0.225m/s and 0.275m/s, the one corresponding to $V_{\text{oil}}^{\text{C2}}$ is the smallest one, and the one corresponding to $V_{\text{oil}}^{\text{C4}}$ is the largest one. Although the flow field makes an oil-spill problem much more complicated than the problem of shooting a solid object, realize that the analogy between them may help us in designing oil boom systems.

Compared to a single boom, this boom arrangement has certainly improved the overall performance in retaining the oil. In the current velocity region $U_0 < 0.24$ m/s ($\text{Fr} < 0.36$), V_{oil} stays very high ($V_{\text{oil}} \geq 0.9$), and it is almost independent of the current velocity. In the region $U_0 > 0.25$ m/s ($\text{Fr} > 0.38$), V_{oil} drops monotonically and smoothly when the current velocity increases. In the curve of V_{oil} vs. Fr, the sharp drop of V_{oil} found in the single boom cases, Fang and Wong (2000), is not found in this case. Without the characteristic point in this region, it is not easy to define a critical Froude number naturally. The critical Froude number is then practically defined as the Froude number under which the boom system can collect 50% of the oil,

$$V_{\text{oil}}(\text{Fr} = \text{Fr}_{cr}) = V_{\text{oil}}(U_0 = U_{cr}) = 0.5 \qquad (6)$$

Under this definition, it is found that this critical Froude number is 0.45, and the corresponding current velocity is 0.3m/s. Up to this point, three velocity regions found in the experiments have been identified in the numerical simulations: In the first region where $U_0 < 0.166$ m/s, more than 50% of the oil is collected in collection zone **C1**. In the second region where $U_0 < 0.24$ m/s, more than 90% of the oil is successfully trapped by the boom system. In the third region where $U_0 > 0.30$ m/s, this boom system is incapable of collecting oil ($V_{\text{oil}} < 0.5$). The three characteristic velocities identified from the numerical results agree well with those obtained from experiments, Wong and Kusijanovic (1999). The satisfactory results indicate the potential for using this numerical model to aid in designing the boom arrangements.

3 System Performance under Different Slope Angles of the Ramp

To optimize the design of a mechanical boom system, it is necessary to change the system's geometry and test its performance after each modification. A complete optimization of the discussed oil boom arrangement is beyond the scope of this study. In this section, we will focus on how the slope of the ramp boom affects this system's performance. Four inclination angles are selected to study for this purpose. The angles (a_{ramp}) of the ramp are 15^0, 25^0, 35^0 and 45^0.

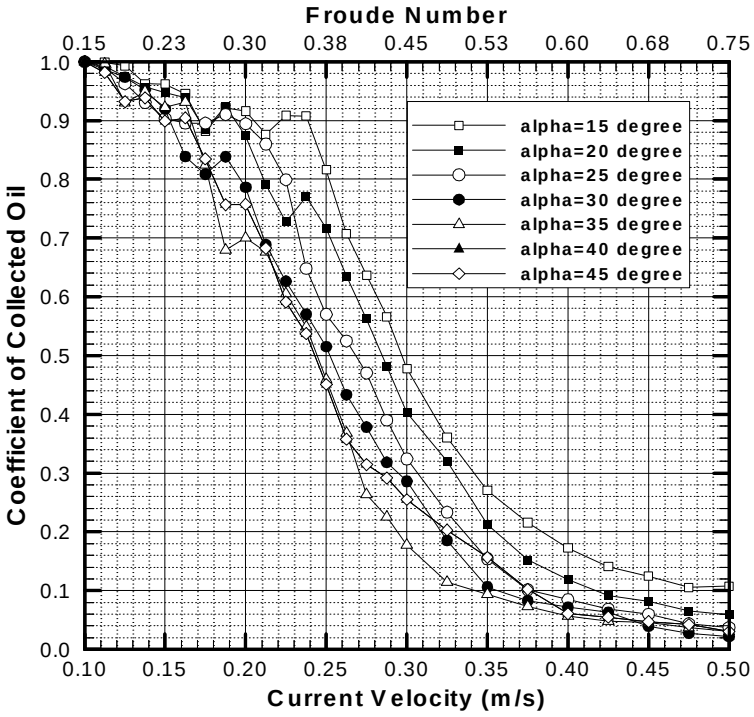

Figure 7 Performance of the boom system under different ramp slopes
Alpha is a_{ramp}, the angle between the ramp boom and the free surface (see Fig.1).

The performances of the modified designs are presented in Fig.7. It is clearly shown that the first design ($a_{ramp} = 15^0$) has the highest coefficient of collected oil (V_{oil}) over all the range of the tested current velocity (U_0). Compared to V_{oil} of the second design ($a_{ramp} = 25^0$), V_{oil} in the first design is higher by about 0.15 when the current velocity $U_0 > 0.23$ m/s. The second design is obviously better than the last two ($a_{ramp} = 35^0$ and 45^0). There is no major difference between the last two designs. When $U_0 > 0.27$ m/s, the fourth design seems better than the third one, but both of them have $V_{oil} < 0.5$.

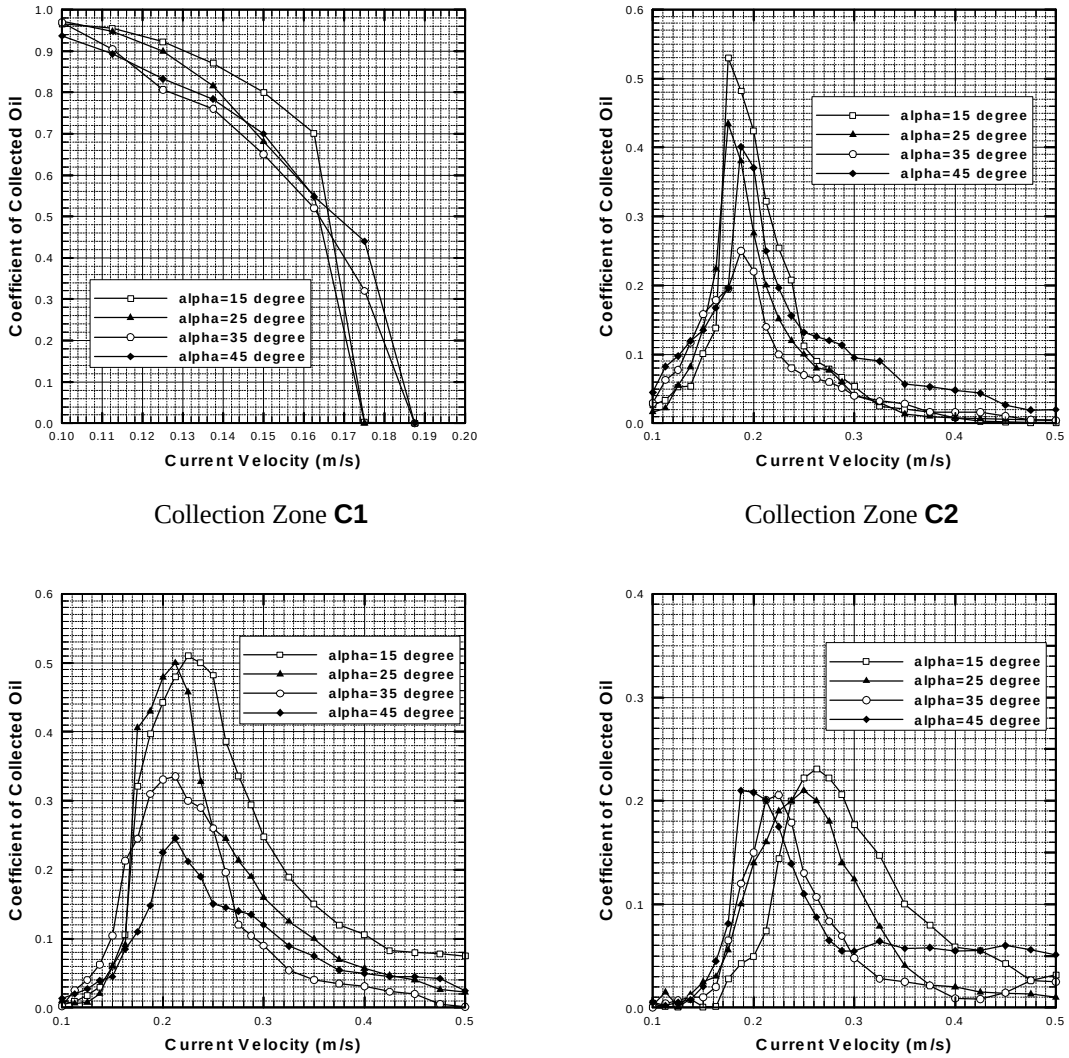

Collection Zone **C1**

Collection Zone **C2**

Collection Zone **C3**

Collection Zone **C4**

Figure 8 Coefficient of collected oil contributed by each collection zone

Alpha is the angle (α_{ramp}) of the ramp boom against the free surface. The definitions of α_{ramp} and Collection Zones are referred to Fig 1.

The portions $(V_{\text{oil}}^{x},\ x = \text{C1}, \text{C2}, \text{C3 and C4})$ contributed by the four oil collection zones are summarized in Fig.8. The curves of $V_{\text{oil}}^{\text{C1}}$ against U_0 are shown in Fig.8(a). It is observed that a design system with a smaller ramp angle may trap more oil in **C1** under a low current velocity, but its $V_{\text{oil}}^{\text{C1}}$ drops to zero earlier and sharper. In spite of these differences, all the $V_{\text{oil}}^{\text{C1}}$s are larger than 0.5 when $U_0 < 0.16$ m/s, and are equal to zero when $U_0 > 0.19$ m/s.

In all the designs with different a_{ramp}, V_{oil}^{x} ($x = \text{C2}, \text{C3 and C4}$) has a similar response characteristic when the current velocity increases from 0.1m/s to 0.5m/s: V_{oil}^{x} increases monotonously to its peak at first, and then decreases. The peak of $V_{\text{oil}}^{\text{C2}}$ occurs when $V_{\text{oil}}^{\text{C1}}$ has just dropped to zero. The current velocity corresponding to the peak is almost independent to a_{ramp}; however, the maximum $V_{\text{oil}}^{\text{C2}}$ decreases when a_{ramp} increases, but there is an exception, the maximum $V_{\text{oil}}^{\text{C2}}$ is very high in the last case ($a_{\text{ramp}} = 45^0$). In **C3**, the maximum $V_{\text{oil}}^{\text{C3}}$ is inversely related to a_{ramp}, and the current velocity corresponding to the peak is also shown to have a weakly inverse relationship to a_{ramp}. The maximum $V_{\text{oil}}^{\text{C4}}$ is likely independent to a_{ramp}, but the current velocity corresponding to the peak is inversely related to a_{ramp}.

Three characteristic regions of current velocity can be found for each design discussed above. The first region, in which more than 50% of the oil is collected by **C1,** can be obtained from Fig.8(a). The second region where $V_{\text{oil}} > 0.9$, and the third region where $V_{\text{oil}} < 0.5$ can be read from Fig.7.

Table 1 Three characteristic regions of the current velocity

Design(a_{ramp})	First region ($V_{\text{oil}}^{\text{C1}} > 0.5$)	Second region ($V_{\text{oil}} > 0.9$)	Third region ($V_{\text{oil}} < 0.5$)
15^0	< 0.166 m/s	< 0.24 m/s	> 0.30 m/s
25^0	< 0.164 m/s	< 0.20 m/s	> 0.27 m/s
35^0	< 0.164 m/s	< 0.17 m/s	> 0.25 m/s
45^0	< 0.168 m/s	< 0.15 m/s	> 0.24 m/s

From the previous discussion, it may be concluded that a smaller ramp slope could achieve a higher performance. Two reasons may contribute to this fact. When the oil slick passes under the ramp boom, the oil flows in the ramp's boundary layer where the shear stress slows down the oil slick. Moreover, the oil movement passing under the ramp boom is against the oil's buoyancy force, which always tends to bring the oil back to the free surface. Because the draft of the ramp is constant, a smaller ramp slope (a_{ramp}) results in a longer length (l_{ramp}) of the ramp boom,

$$l_{\text{ramp}} \propto 1/\sin(a_{\text{ramp}}) \tag{7}$$

A longer ramp boom gives the shear stress and buoyancy force more action time, So a smaller ramp angle results in a lower "throwing velocity" (u_t), defined at the bottom of the ramp. According to the trajectory theory, the "landing distance" (D_l) is

$$D_l = u_t^2 \sin(2a_{\text{ramp}})/g_r \tag{8}$$

where g_r is the reduced gravity in this case. It is clear that when $a_{\text{ramp}} < 45^0$, both u_t^2

and $\sin(2a_{\text{ramp}})$ decreases when a_{ramp} decreases, so does D_l. A small landing distance is essential for this boom arrangement to practically achieve a high performance. However, a very small ramp is practically unacceptable due to its large size. For example, the length of the ramp is 3.86 times of its draft at $a_{\text{ramp}} = 15^0$, but this length enlarges to 7.66 times of the draft at $a_{\text{ramp}} = 7.5^0$.

4 System Performance under Tide Conditions

With the presence of waves, the oil begins to escape much earlier than predicted by the studies in which the surface waves are neglected (Kordyban, 1992). In the present numerical model, the wave elevation at the free surface is assumed to be very small, and the effect of the surface wave cannot be simulated. But by imposing time-dependent incoming current conditions, we may gain insight about the performance of the boom arrangement under tide conditions.

We select the boom arrangement with $a_{\text{ramp}} = 15^0$, and the mean incoming current velocity with $U_0 = 0.25$ m/s. Referring to the curve of V_{oil} presented in Fig.6, one may find that the selected parameter set is in the sensitive region, V_{oil} would be very sensitive to changes in current velocity. The incoming velocity is modeled as

$$u_0 = U_0[1 + a\sin(wt)] \tag{9}$$

where a is called the amplitude of tide, U_0 is the mean incoming velocity. In the numerical simulations, ten values are assigned to this amplitude, from 0.1 to 1.0 at increments of 0.1. w is the angular frequency of the tide.

$$w = 2p / T_w \tag{10a}$$

where T_w is the period of the tide. The dimensionless w is

$$w = 2pd / U_0 T_w \tag{10b}$$

where $d = 4.5$ cm is the draft of boom A (or B).

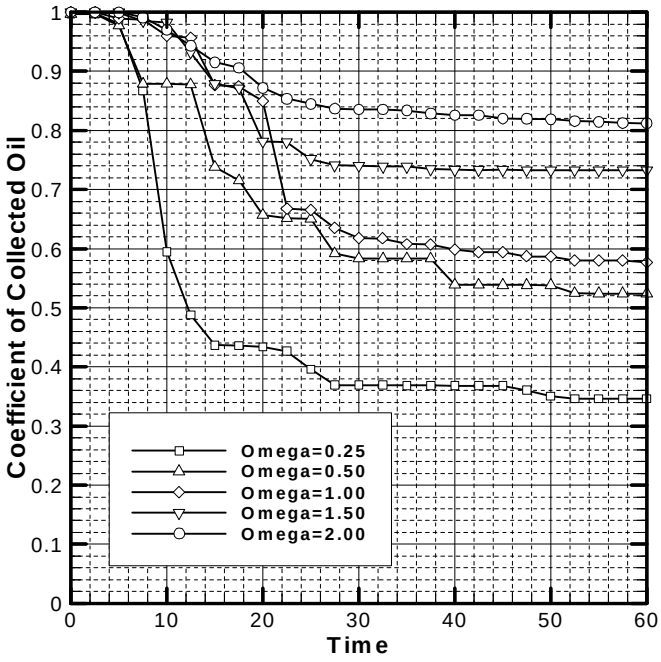

Figure 9 Coefficient of collected oil vs. time ($a = 0.5$)
Omega (w) is the dimensionless angular frequency of the tide current. $w = 0.25$ corresponds to the tide period of 4.5 seconds; $w = 2.00$ corresponds to the tide period of 0.57 second. The unity of the dimensionless time corresponds to 0.18 second.

Suppose that the period of the tide is in the range between 0.5s and 4.0s in the laboratory experiment. Then the dimensionless parameter w is in the range between 2.26 and 0.28, calculated by Eqn.10a. In the simulations, five values are then assigned to the dimensionless w, which are 2.0, 1.5, 1.0, 0.5 and 0.25.

It is shown in Fig.9 that the coefficient of collected oil changes with time. The amplitudes of the tide are 0.5 in all five curves. The first observation regarding the coefficient of collected oil at time=60 is that the larger the angular frequency w, the higher the system's performance (V_{oil}), and the earlier the final V_{oil} is reached.

In the cases with $w \le 1.5$, it is found that V_{oil}s are stepped down before they reach their final values, and the times of the drop in V_{oil}s occur near the peaks of the tide velocities. Only in the last case with $w = 2.0$, the curve is smooth. But in this case, the tidal period is 0.57 second, while the interval between two adjacent data presented in Fig.9 is 2.5×0.18 second $= 0.45$ second. The data interval is not fine enough to catch the steps even if they exist.

Oil is lighter than water, it tends to float to the free surface, and oil's viscosity is usually higher than that of water; this means that an oil slick cannot follow the periodic movement of a tidal current. In this sense, the oil's movement inside the oil collection zones is analogous to the movement of the heavier objects in a sifter. The appropriate amplitude and angular frequency of a tide may send more oil into the oil collection zones. This deduction has been proved by the fact presented in Fig.10. Around the tide

amplitude $a \approx 0.1$ (there is an exception with the case $w = 0.5$, in which $a \approx 0.2$), it is observed that the coefficient of collected oil reaches its maximum, which is even greater than that in the case without a tide ($a = 0$). After this point, in the case with small w the performance becomes worse when the amplitude increases; while in the case with $w \geq 1.5$, a plateau of V_{oil} exists when the tide amplitude is in the range $0.2 \leq a \leq 0.5$.

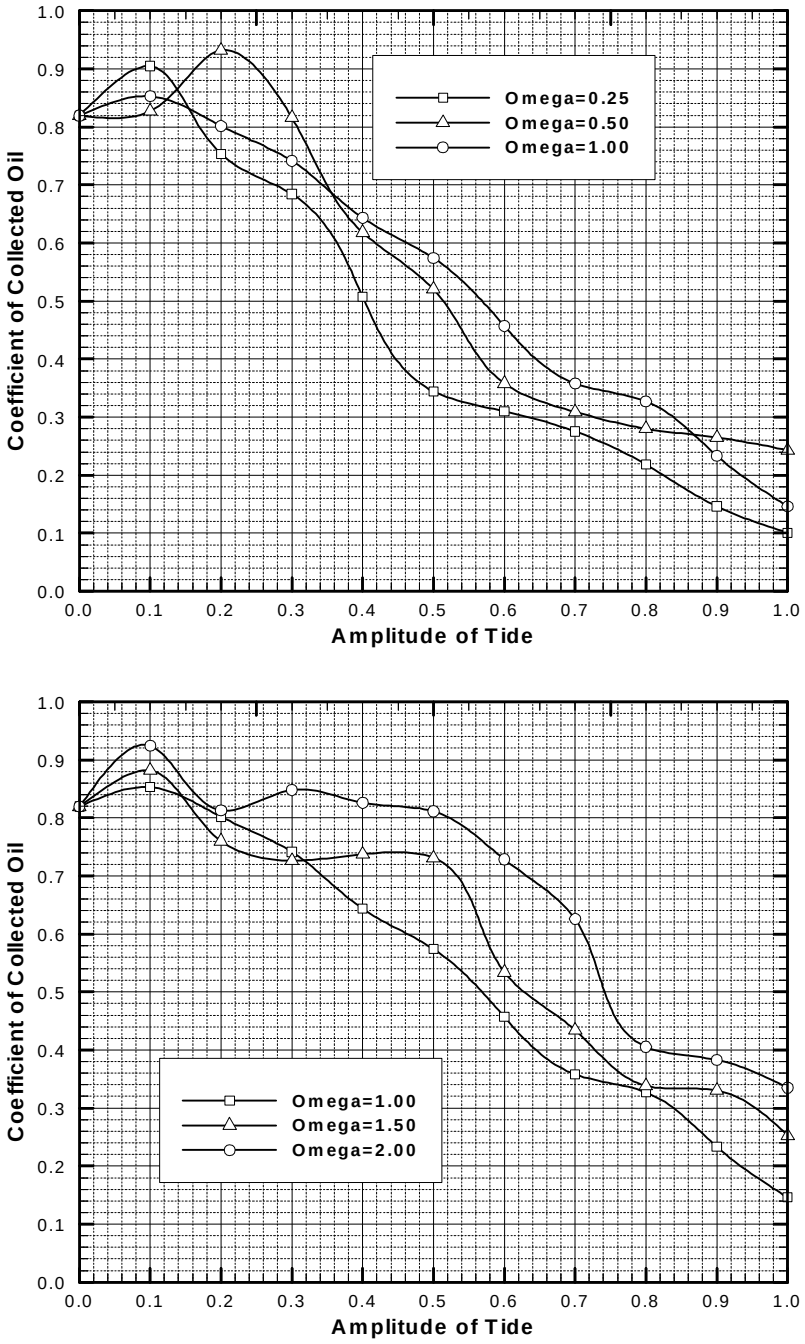

Figure 10 Coefficient of Collected Oil vs. Amplitude of Tide

Omega (w) is the dimensionless angular frequency of the tide current. $w = 0.25$ corresponds to the tide period of 4.5 seconds; $w = 2.00$ corresponds to the tide period of 0.57 second.

Conclusion

In this paper, we present the numerical study of a particular oil boom arrangement. Under the given parameters, it is concluded as follows:

1. This boom arrangement has a better performance compared to a single oil boom.
2. The oil slick flowing under the ramp boom is similar to a solid projectile travelling under the influence of the gravity. To achieve a high performance, the ramp slope should be as small as possible, and the span of the boom system should cover the "landing point" of the oil.
3. A small amplitude tide may improve the system's performance, while a large amplitude tide significantly deteriorates it. A smaller angular-frequency tide is more harmful to the system, especially when the amplitude of the tide is also large.

References:

Delvigne, G. A. L., Laboratory experiments on oil spill protection of a water intake, Delft Hydraulics Laboratory, Publication No.328, Delft, the Netherlands, 1984.

Delvigne G. A. L., Barrier failure by critical accumulation of viscous oil, Proceedings of Oil Spill Conference, USEPA, USCG, and American Petroleum Institute, pp.143-148, 1989.

Ertekin, R. C. and H. Sundararaghavan, The calculations of the instability criterion for a uniform viscous flow past an oil boom, Journal of Offshore Mechanics and Arctic Engineering, vol.117, pp.24-29, 1995.

Fang, J.Z. and K.V. Wong, An advanced VOF algorithm for oil boom design, International Journal of Environment and Pollution (Accepted), 1999.

Fang, J.Z. and K.V. Wong, Instability study of oil slicks contained by a single boom, Proceedings Twenty-Third Arctic and Marine Oil Spill Program Technical Seminar, Vancouver, Canada, 2000.

Fang, J.Z, Instability study of oil slicks contained by oil boom systems, Ph.D. Dissertation, University of Miami, 2000.

Ingham, D. B., T. Tang and B.R.Morton, Steady two-dimensional flow through a row of normal flat plates, Journal of Fluid Mechanics, Vol.210, pp.281-302, 1990.

Johnson, R. W., The handbook of fluid dynamics, CRC Press LLC, 1998.

Johnston, A. L., M.R. Fitzmaurice and R.G.M. Watt, Oil spill containment: viscous oils, Proceedings of Oil Spill Conference, USEPA, USCG, and American Petroleum Institute, pp.89-94, 1993.

Leibovich, S., Oil slick instability and the entrainment failure of oil containment booms, Journal of Fluid Engineering, Vol.98, pp.98-105, 1976.

Lo, J. M., Laboratory investigation of single floating booms a and series of booms in the prevention of oil slick and jellyfish movement, Ocean Engineering, Vol.23, No.6, pp.519-531, 1996.

Wong, K. V. and Kashyap, R., Estimating the Burn Rate from the Boom Configuration,

Proceedings 17th AMOP Technical Seminar, Vol.2, Canada, 1994.

Wong, K. V. and Guerrero, D., Quantitative analysis of shoreline protection by boom arrangements, Proceedings Second International Oil Spill R&D Forum, London, U.K, 1995.

Wong, K. V. and A.Wolek, Application of flow visualization to the development of an innovative boom system, Proceedings Nineteenth Arctic and Marine Oil Spill Program Technical Seminar, Calgary, Canada, 1996.

Wong, K. V. and I.P. Kusijanovic, Oil spill recovery methods for inlets, rivers and canals, International Journal of Environment and Pollution (Accepted), 1999.

Wong, K.V. and L. Hernandez, Arrangements of collection devices to better gather spilled oil, International Journal of Environment and Pollution (Accepted),1999.

Acknowledgements

This work was funded in part by the Minerals Management Services. Thanks go to Mr. Jim Lane of M.M.S.